Journal of Basic Physical Research ISSN: 2141-8403 Prints, 2141-8411 Online
Vol.8, No.2 pp. 1- 18, July, 2018. Available online at www.jbasicphyres-unizik.org

SHALLOW-SURFACE 2DERT SURVEY AT THE VICINITY OF URUAGU-NNEWI GULLY SITE, ANAMBRA STATE

Agarana, D. C. and Egwuonwu, G.N.
Department of Physics and Industrial Physics, Nnamdi Azikiwe University, Awka
Email: gn.egwuonwu@unizik.edu.ng

Abstract
Geoelectric survey has been carried out at the vicinity of an active gully site in Uruagu, Nnewi, Anambra state, Nigeria in order to delineate the lithology and subsurface geologic structures therein suspected to be prone to failure. Electrical Resistivity Tomography (ERT) data was collected based on Wenner array with the aid of ABEM SAS 1000 terrameter and multi-electrode selector ES10-64. Forty-two steel electrodes were aligned concurrently for the automated selection of four-electrode system of Wenner32SX protocol for each datum point measured. The registered data were processed with the aid of Res2DInv Version 3.2 software. Results of the shallow-surface 2D model inversion tomograms showed that the resistivity range of the eight selected profiles falls between $1\ \Omega m$ *to* $25{,}500\ \Omega m$*. Interpretation of this range based on the geologyy of the area, previous works at the study area and published standard resistivity, the range of resistivity in the area encompasses that of weathered laterite, saturated soil, clay, sandy clay, clayey sand and sandstones occurrences at depths. Of these, clay, sandy clay and clayey sand of various grades were noted to be predominant. Structurally, the tomograms show a moderate heterogeneity, minor portions of relatively flat layering, suspected fractured and anticlinal zones at depths. The study suggests that the active landslides currently exacerbated at Uruagu-Nnewi are most probably aggravated by differential saturation of the shallow gully's vicinity hence, leading to intermittent abrupt landslide and failures. The understanding that the immediate vicinity of Uruagu-Nnewi gully site is predominantly characterised by saturated, weak and aqueous clayey soils is undoubtedly a vital information to curious environmental managers. Particularly, civil engineers are richly informed about the unseen depths of the gully's vicinity from the foregoing findings and would be well guided in their foundation designs for construction works towards erosion control and bridges at the site. Hence, the menace can be said to have been proactively and ultimately be resolved based on this near-surface geophysical survey.*

Introduction
Soil erosion is the loosening or the process of detachment and consequent removal or transportation of soil materials from one location to another by agents of erosion such as wind, water or ice (Ezeigwe, 2015). Gully erosion, the most striking erosion type, has been recognized as one of the major global environmental problems (Abdulfatai *et al.*, 2014). It is the most obvious form of soil erosion and very conspicuous because of the remarkable manifestations of the physical loss of land, landslides and superstructures' failure associated with it. Of all kinds, gullies which are obviously consequential to erosion are of different types, vis-à-vis base level, scarp, fracture and incidental (Ezechi and Okagbue, 1989). Table 1 shows the various modes, conditions of formation and common advance mechanism of gully types.

Table 1: Gully types, modes and conditions of formation and common advance mechanism (Ezechi and Okagbue, 1989).

Gully Type	**Modes and Condition of Formation**	**Common Advance Mechanism**
Base level	Groundwater flow.	Slope undermine, sliding and slumping.
Scarp	Runoff and slope change.	Slope undermining, sliding/slumping, toppling.
Fracture	Runoff and shrinkage fracture.	Collapsing, also block failure.
Incidental	Runoff concentration and vulnerable soil exposure by man.	Common sliding/slumping.

Gullies could also be described in terms of shape; either U or V-shaped, or in terms of dimension and sizes small, medium and large. Most U-shaped gullies are noted with depths varying from 3.5

m to 400 m, widths on the range of about 4.2m to 5,700m and lengths between 32m and 7,100m, respectively (Riyadh, 2014). Some gullies could be very deep having their associated failure defies moderate control measures. Such gullies are noted to most likely be resulting from the interplay of exogenic and endogenic forces (Riyadh, 2014). Landslide is also noted to describe rapid forms of mass wasting; downslope movement of earth materials under the influence of gravity. Mass wasting during a landslide event strongly depends on topography of the ground, hydrology, the structure and type of underlying bedrock, soil and other factors (Jadwiga *et al.*, 2012).

Gravity acts on all bodies on Earth's surface. There are two components for bodies or objects resting on sloping surfaces. While one component (g_s) is parallel to the slope, the other (g_p) is perpendicular to it. On steep slopes (usually greater than >45^o), the component parallel to the slope are greater and will act to pull objects downhill. On gentle slopes, the components perpendicular to the slope are greater and will act to hold the object in place (Nelson, 2015). Figure 1 shows the components of gravity oriented parallel and perpendicular to the slope for both gentle and steep slopes.

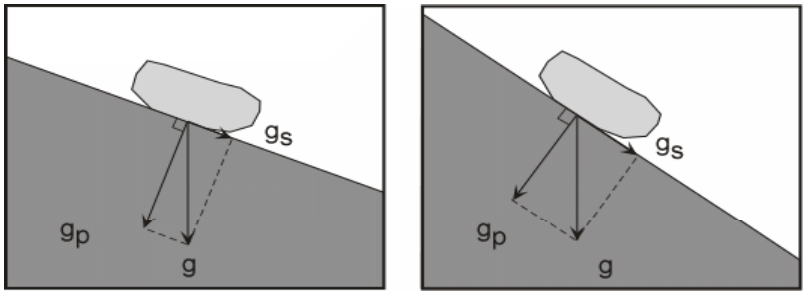

Fig.1: Components of gravity oriented parallel (gs) and perpendicular (gp) to the slope for gentle and steep slopes (Nelson, 2015).

However, gravity alone does not determine if the object will move downslope. A physical trigger is often required to initiate slope failure. Addition of excess water to a slope may also be the precursor for a disaster. Not only does excess water saturate materials and reduce cohesion between grains but water-saturated pore spaces will support the weight of overlying material thus reducing the effect of friction. So, the addition of water may promote instability by adding weight to a slope (Watkins and Hughes**,** 2000). The macroscopic manifestation of erosion and landslide occurrences at some areas is subjected to certain factors. These include; the geology of the area, land use act, geomorphology, climate, soil texture, nature and bio diversity of the area (Riyadh, 2014). At some areas, landslides occur mostly due to earth movement, rock and debris flows on slopes previously weakened by flood water (Igbokwe *et al.*, 2008).

High hydrostatic pressure in the aquifer produces a reduction in the effective strength of the unconsolidated lease sands in the walls of the gullies leading to intense erosion/landslide (Riyadh, 2014). Significantly, water plays a role in landslides, other factors such as earthquakes, the presence or absence of vegetation, and human activities (such as logging may remove vegetation that shelters the slope) can also influence the potential for landslide (Watkins and Hughes, 2000). Runqiu and Weile (2011) also showed in their work that topography, tectonics, lithology and climate are some phenomenon that can cause landslides. They also listed landslide-triggering factors to mainly include rainfall, human activities, snowmelt, earthquakes, reservoir impoundment, typhoons, volcanic eruptions, etc. Human activities disturb large volumes of earth materials in construction of buildings, transportation routes, dams and reservoirs, canals, and communications systems, and thus have been a major factors causing slope failures (Robert and Lynn, 2001). But of all these, rainfall and earthquakes are the two most predominant

triggering factors of landslides (Runqiu and Weile, 2011). Environmental disturbances are results of general tendency toward degradation of the Earth's surface by gravitational mass wasting and erosion (Robert and Lynn, 2001). Multiple on-site and off-site effects of gully erosion/landslides threaten sustainable development, which is especially evident in dry land environments (Frank *et al*., 2014). These processes may be slow and gradual or swift and deadly (Jadwiga *et. al*., 2012).

The Study Site

The study site lies within latitudes $06°00'58''N$ to $06°01'14''N$ and longitudes $06°54'32''E$ and $06°54'47''E$ at an average elevation of 90.83 m above the mean sea level. The area is underlain by cretaceous to recent sedimentary formations of Anambra basin of Nigeria which have varying aquifer potentials (Uzoije *et. al*., 2013). Nnewi area wherein the study site location is characterized by Ameki Formation. It is sitting directly on the flange of lignite series underlain by Bende Ameki Formation (Onochi and Ibearugblem, 2012). The Bende Ameki Formation was deposited during the middle Eocene of the Tetiary period. It consists of series of highly fossiliferous greyish green sandy clay, calcerous concretions and white clayey sandstone. Two lithological groups have been identified in parts, the lower with fine to coarse sandstone and thin shaley limestone, the upper with coarse cross-bedded sandstone bands of fine grayish green sandstone and sand clay (Onochi and Ibearugblem, 2012). Greater part of the study area is made of Plateau and ridges. This is a part of the higher Plateaus that extends from Enugu towards southeast of Anambra State of Nigeria, and has the characteristics of dissection and marginal ridges that consists of small low lands. The soil consists of moderately drained sands, silt and sandy clay with top layer of black to brownish humus and laterite (Uzoije *et. al*., 2013). Uruagu Nnewi (Figure 2) has lignite formation with thick beds of sand, clay and contains seams of lignite. The thickness ranges up to 300m in some places. (Onochi and Ibearugblem, 2012).

The widespread impact of gully erosion resulting from annual rainfall and subsequent flooding leads to the occurrence of landslides in different parts of south-eastern Nigeria. The rainy season registers an average annual rainfall of 2000 mm (Egboka and Okoyeh, 2016). Observations have shown clearly that gully erosion is the major cause of landslides in Nigeria and it is more prevalent in sedimentary terrain than in the basement complex of Nigeria, Anambra State being the most affected of all the states in Nigeria with Agulu, Nanka and Oko communities of the state the worst hit (Abdulfatai*et al.*, 2014).

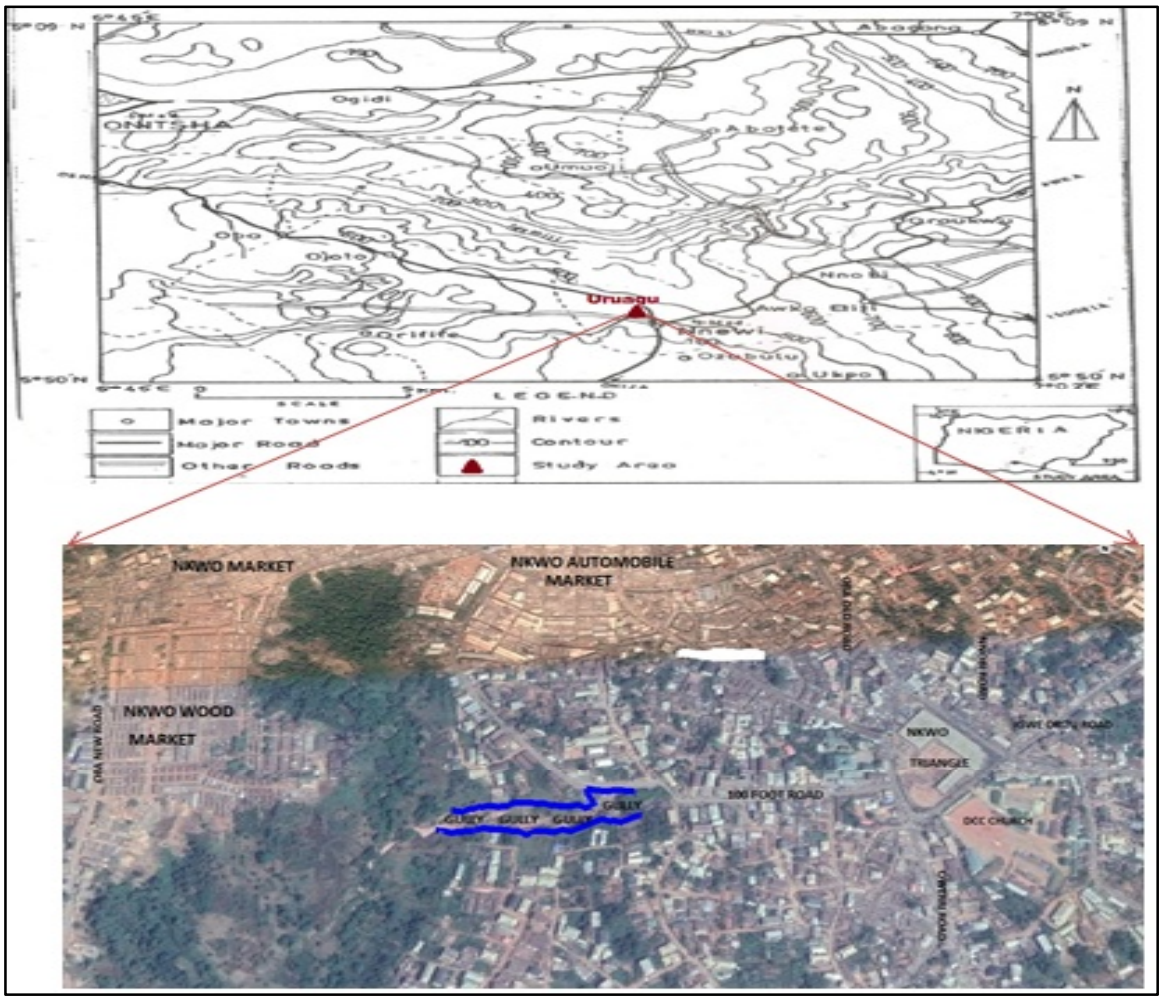

Fig.2: Map of the study area, gully site and the surrounding (modified from Uzoije et al., 2013; Google Map, 2018).

The menace has taken its toll on the socioeconomic wellbeing of the people living in the affected area and the country at large such that lands used for aesthetic, agricultural and industrial purposes, ancestral homes, crops, livestock and other infrastructure are everyday being lost to the hazard at alarming rate (Obiadi *et al*., 2011). Investigations carried out by Egboka and Nwankwo (1982) showed that the causes of gully genesis and growth may lie in the hydrogeological and geotechnical properties of the aquifer system underlying the areas being affected. Uruagu-Nnewi gully site has been noticed to be actively progressing for the past decade. Prior to the reconnaissance survey of this study, the expansion and failure of the gully encroached towards few buildings close to its boundary. These subsequently fell into the gully and typical of this is shown in Figure 3. Also, in the course of the study was occurrence of the expansion of ground surface cracks on the major road at the Uruagu-Nnewi gully site's vicinity which eventually fell rendering the road unusable (Figure 4).

Fig.3: The Active and Progressive Gully Site at Umudim, Uruagu Nnewi, Anambra, Nigeria

Fig.4:The Gully Encroaching a Major Road

This study is therefore aimed at unravelling the causes of the current and impending shallow-surface failure at Uruagu-Nnewi gully site. This detailed understanding of the internal structure of the gully's vicinity would serve as fundamental information for mitigating the risk at the area, thus providing intended civil engineering works with useful data for checking the near-surface menace.

Methodology

Tomography is an imaging technique which generates a cross-sectional picture of object(s) by utilizing the object's response to a non-destructive, probing energy of an external source (Tien-When and Philip, 1994). When the probing energy is electrical, delineating resistivity of the material, it is called Electrical Resistivity Tomography (ERT), otherwise, called Electrical Resistivity Imaging (ERI). ERT involves the acquisition of resistivity data by the injection of current into the ground via a pair of electrodes and then the resulting potential field is measured by a corresponding pair of potential electrodes. Electrical resistivity tomography has also been found to be time saving and more accurate subsurface modelling technique. 2D ERT survey measures the resistivity changes both in the vertical direction (sounding), as well as in the horizontal direction (profiling) along common survey line at the same time. 2D electrical imaging doesn't only give more accurate results and save time, it is also cost effective. While the 1-D resistivity sounding surveys may involve few readings, 2D imaging surveys involve about 100 to 1000 measurements (Egwuonwu, 2012).

Instrumentation

The resistivity instrument used in this survey is ABEM LUND Imaging System namely, Terrameter model SAS 1000.The basic accessories are the multiple stainless steel electrodes, reels and cables, an electrode selector model ES 10-64. The system is unique because its ammeter and voltmeter measure the current and voltage combined in a single meter reading resistance. The computerized Terrameter meant for the data collection processes the resistivity of each point measured in the subsurface. Figure 5 shows the ABEM LUND imaging system and its accessories used for the survey. The instrument is powered by a clip-on NiCd battery pack or by an external 12 volts source which clips conveniently onto the bottom of the instrument. An alternative to the external battery adapter (SAS-EBA) is any other external 12 volts D.C. source equivalent to vehicle accumulator (ABEM, 2010).

Fig.5: The ABEM Lund Imaging System and Accessories (ABEM, 2010)

Field Work

The fieldwork was carried out at the vicinity of a gully site actively developing at *100-foot road,* Umudim, Nnewi in Anambra State, Nigeria. The data collection was at the peak of dry season in order to ascertain the minimum saturation of the near-surface soils and rocks at the site. Precisely from 17th to 24th March, 2018 after a reconnaissance study on the 10th of the same month. This period was also chosen in order to avoid disturbances by rainy season which would have either slowed down the work or endangered the safety of the instrument due to thunderstorm. Eight profile lines were mapped for measurement whereupon 2D resistivity imaging was conducted. Four survey lines were relatively oriented in E-W direction namely profile 1(P1), profile 4(P4), profile 6(P6)and profile 8(P8) whereas the other four survey lines were relatively oriented in S-N

direction namely profile 2(P2), profile 3(P3), profile 5(P5), profile 7(P7) (Figure 6). Based on the availability of space at the built up area, P2, P3,P5, P7 and P8were dimensioned 84m in length whereas the P1, P4andP6 were126m in length. The electrodes spacing used at each profile line were based on the limit of space provided at the site which is highly confined. Secondly, the spacing was based on the maximum takeout spacing (2 m) on the reel cables provided. Measurements for each profile line took between 35 minutes and 50 minutes for the range of about 160 to 190 datum points. Precautionary measures such as avoidance of proximity to high voltage cables and transformers and avoidance of stray animals from getting in touch with the instrument were taken. Overheating of the instrument was also avoided thus, it was ensured that the instrument was not exposed to direct sun with the aid of field umbrella and operated in a well ventilation place. In order to avoid abrupt stoppage of measurement in the imaging system during the field work owing to low battery e.m.f., a 12 Volts back up fully charged was provided.

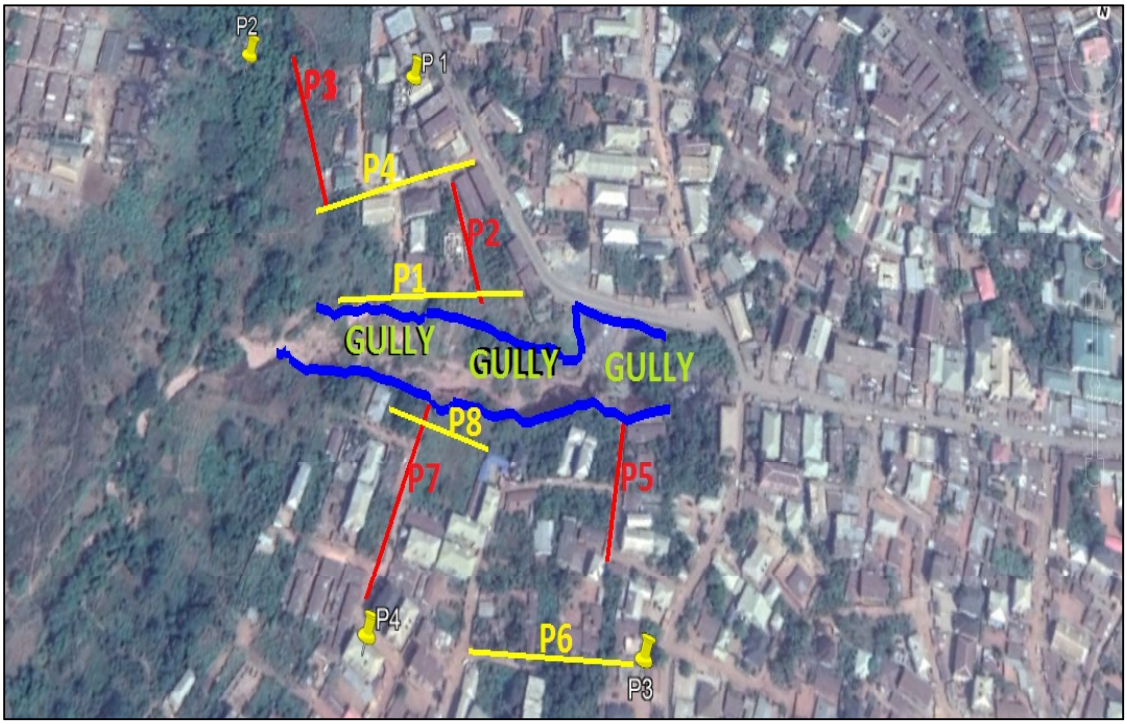

Fig. 6: Google Earth Image of Study Area Showing the Eight (8) profiles (modified after Google Earth, 2018)

The forty-two (42) electrodes were connected to all the take-outs at intervals predetermined for each profile on the cables using jumpers. When powered for measurement, the network with ES 10-64 automatically switched on, did both the profiling and sounding measurements using the setting of Wenner 32SX protocol array in the Terrameter.The programme automatically continues to measure using the two electrode cables when the contact is satisfactory.While measuring the profiles, reference coordinates namely latitudes and longitudes of the two ends of the profiles were noted for identification during interpretation (Table 2).

Table 2: Coordinates, Length and orientation of the two ends of the Profile Lines

Profile	Point 1		Point 2		Profile Length (m)	Orientation
	Latitude	Longitude	Latitude	Longitude		
P1	$6^0$00'58"N	$6^0$54'41"E	$6^0$00'56"N	$6^0$54'39"E	126	S80^{0}W
P2	$6^0$01'04"N	$6^0$54'34"E	$6^0$01'03"N	$6^0$54'39"E	84	N40^{0}W
P3	$6^0$01'06"N	$6^0$54'36"E	$6^0$01'03"N	$6^0$54'37"E	84	N40^{0}W
P4	$6^0$01'01"N	$6^0$54'32"E	$6^0$01'08"N	$6^0$54'37"E	126	S80^{0}W
P5	$6^0$01'06"N	$6^0$54'46"E	$6^0$01'03"N	$6^0$54'46"E	84	S20^{0}E
P6	$6^0$01'01"N	6°54'40"E	$6^0$01'01"N	6°54'47"E	126	N85^{0}E
P7	$6^0$01'05"N	6°54'41"E	$6^0$01'02"N	6°54'41"E	84	S5^{0}W
P8	$6^0$01'14"N	$6^0$54'44"E	$6^0$01'03"N	$6^0$54'46"E	84	N87^{0}W

Having carried out field work using 2D model resistivity, the data were processed and with the aid of Res2DInv software the tomograms were generated. The models of the data were interpreted based on the knowledge of standard resistivity, previous work done close to the area and based on the geology of the area.

Data Processing

Interpretation of the results from electrical imaging was preceded by adequate data processing of the raw data using the Res2DInv software. Before the processing of the resistivity data registered from the survey, the raw data of the apparent electrical resistivity collected was downloaded to a computer system wherein the ABEMSAS 1000 Terrameter utility software has already been installed. The raw data files were first converted to *.dat* format. A laptop with minimum available memory space of 40GB, with adequate RAM and processor speed was considered fast enough in iterating true colour pseudosection of resistivity values. Robust Smoothness constrain inversion was performed during its automatic model interpretation using finite difference forward modelling and quasi-Newton techniques (Loke, 1994).

The inversion resistivity model blocks were plotted in such a way that the calculated apparent resistivity plots agreed with the plots of the measured field data. The system executable file namely Res2dInv.exe automatically subdivides the subsurface into number of blocks and used a least–squares inversion scheme to determine the appropriate resistivity value for each model block. Using some auto default parameters, data was converted before the inversion process. The least–squares inversion converts the measured apparent resistivity values to true resistivity values and plotted them in cross-section. It first creates a resistivity cross–section, calculates the apparent resistivities and compares the calculated with the measured apparent resistivities. If the discrepancy is much, the iteration repeats until the minimum discrepancy is reached. Hence data quality was improved upon for a reliable model when observed to be poor. After the data download from Terrameter to laptop, editing the data was carried out whereupon changes were enabled on the data that was read from the input data file. That is, there was removal of the bad data points and selection of portion(s) of the data set to invert were made. Figure 7 shows the data set with a few bad points for Profile 1 of this investigation which were removed.

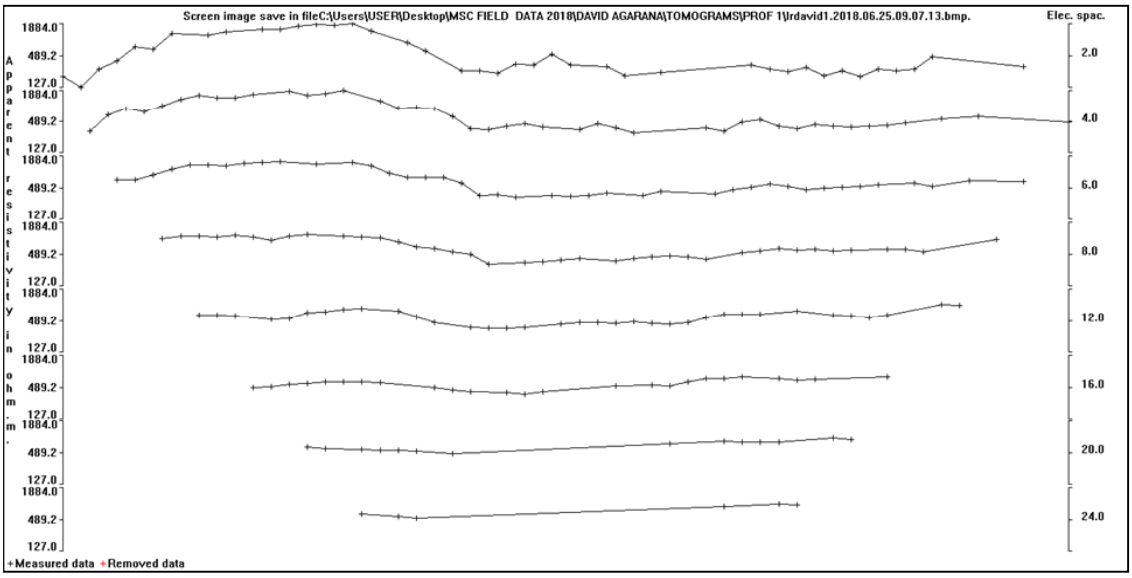

Fig.7: A Profile Showing the Data Set of Profile 1with a few Bad Data Points Removed

Other changes such as splice large data set, reversals of pseudosections, changing of the location of first electrode and editing data file were not considered necessary during the data processing. Changing of the programme settings, inversion of damping parameters namely; damping factor with depth, optimization of damping factor, limiting the range of model resistivity, change in vertical to horizontal flatness filter ratio were all left at the programme's set default. Also the provision for change in the finite-difference mesh parameters used in the forward modelling subroutine was not altered from their defaults. Inversion constraints used to control the path the inversion subroutine took during the inversion progress for each data set were also left at their set defaults. These include the line search and its percentage change, convergence limit (left at 5%) for the relative change in the RMS error between 2 iterations. model resistivity values check and the number of iterations were set at default for a demo version of the software which is three. Finally, data display selection was set at a considerate cut-off limit and contour intervals of pseudosections at the data processor's inversion parameters.

Inversion Options such as model blocks and Smoothing of model resistivity values used for the inversion and the change in some of the parameters that regularize the inversion were ensured adequate before inversion. Hence the least-squares inversion routine was started. The least-squares formulation using the smoothness constraint on the model perturbation vector produced models with a reasonably smooth variation in the resistivity values. For noisy data sets, better results were obtained by the application of a smoothness constraint on the model resistivity values as well. Defaults of the discretization were allowed on the model block display mode, thickness of the model layers, and the number of the data points which were not extended to the edges of the sections by default.

Finally, in displaying the inversion results, all the data output file produced by the inversion subroutine namely the measured, the calculated and the model (inverted) apparent resistivity pseudosections were displayed. Little changes were made on the contour interval used for drawing the pseudo and model sections. At the window display pseudosections and model sections, the widow section was entered; the detail of the iteration which has generated the model data and sections appeared (Figure 8). The numbers of sections to display were specified and by defaults, all the observed, calculated apparent resistivity model pseudosections were displayed.

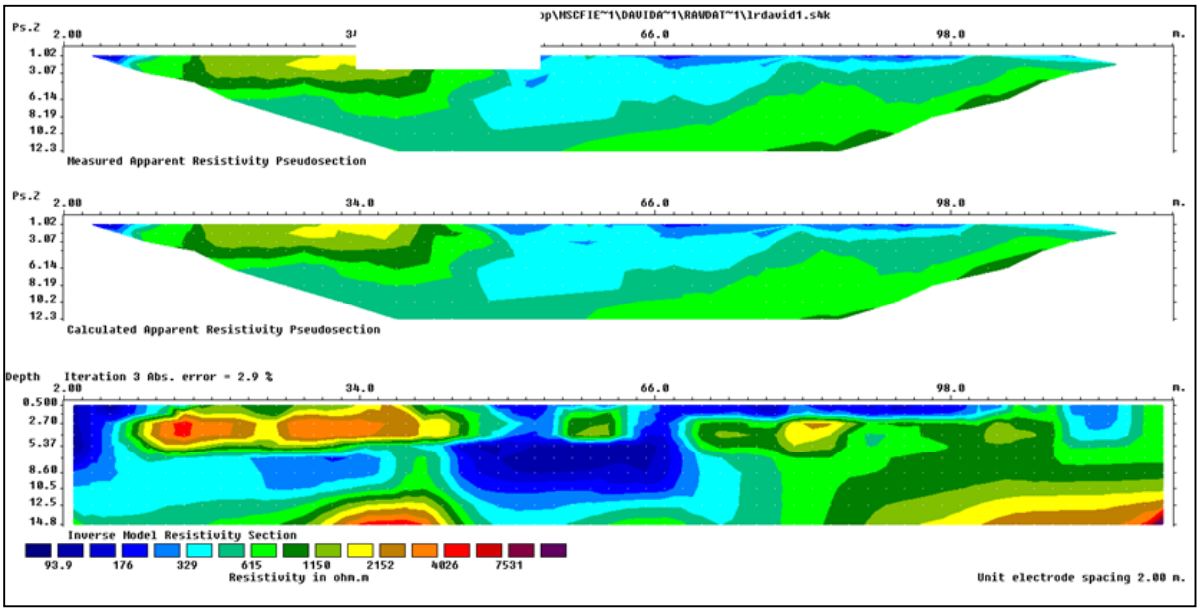

Fig.8: The Result of 2D Inversion of the Wenner Array Data along Survey Profile 1, (a) The Observed Data Plotted as a Pseudosection; (b) The Calculated Pseudosection and (c) The Inverse Model Showing the True Depth and True Formation Resistivity.

7.0 Mathematical theory/background

The difference between the observed data and the model response is given by the discrepancy vector g that is defined by (equation 1) was reduced to the bare minimum.

$$g = y - f \tag{1}$$

Where y is the set of the observed data and f is the model response. Using the least-squares optimization method, the initial models were modified such that the sum of square errors E(equation2) of the difference between the model response and the observed data values is minimized.

$$E = g^T g = \sum_{i=1}^{n} g_i^2 \tag{2}$$

To reduce the above error value, Gauss-Newton equation (equation 1) is applied to determine the change in the model parameters that should reduce the sum squares error (Lines and Treitel, 1984).

$$J^T J \, \Delta q_1 = J^T g \tag{3}$$

Δq_1 is the model parameter change vector, and J is the Jacobian matrix.Problems of unrealistic values was avoided based on common method of the Marquardt-Levenberg modification (Lines and Treitel, 1984) to the Gauss-Newton equation (equation 4) and is given by;

$$(J^T J + \lambda I)\Delta q_k = J^T g \tag{4}$$

I is the identity matrix and the factor λ is the Marquardt or damping factor. Equation 4 defines the ridge regression method (Inman, 1975) which was used in the inversion of resistivity sounding data and the model consists of a small number of layers. However, in situation where the number of model parameters is large in the 2D inversion model, the model produced by this method may have an erratic resistivity distribution with spurious high or low resistivity zones (Constable *et al.*, 1987). Therefore, the Gauss-Newton least-squares equation was further modified so as to minimize the spatial variations in the model parameters to overcome this problem to overcome this problem. That is, the model resistivity values change in a smooth or gradual manner. This smoothness-constrained least-squares method (Ellis and Oldenburg 1994a) is given as;

$$(J^T J + \lambda F)\Delta q_k = J^T g - \lambda F q_k \tag{5}$$

Where $F = \propto_x C_x^T C_x + \propto_y C_y^T C_y + \propto_z C_z^T C_z . C_x$, C_y and C_z are the smoothing matrices in the x-, y- and z-directions. $\propto_x$, $\propto_y$ and $\propto_z$ are the relative weights given to the smoothness filters in the x-, y- and z- directions. Equation (5) is the least square l_2 norm smoothness-constrained optimization method which produce a model with a smooth variation of resistivity values. Least absolute deviation l_1 norm smoothness-constrained optimization method is blocky inversion method applied where the subsurface geology is suspected to consist of a number of regions that are internally almost homogeneous but with sharp boundaries between different regions. For such cases, the inversion formulation was modified in order to minimize the absolute changes in the model resistivity values and to give significantly better results (Claerbout and Muir, 1973, Loke, 2004, Wolke and Schwetlick, 1988). The optimization equation in (5) is then modified to

$$(J^T J + \lambda F_R)\Delta q_k = J^T R_d g - \lambda F_R q_k \tag{6}$$

with $F = \propto_x C_x^T R_m C_x + \propto_y C_y^T R_m C_y + \propto_z C_z^T R_m C_z$ where R_d and R_m were weighting matrices introduced so that different elements of the data misfit and model roughness vectors are given equal weights in the inversion process. Equation 6 provides a general method to further modify but was not found necessary in this work.

Some sources of errors avoided include; garbage-in garbage-out of unusually low or high apparent resistivity values, non-uniqueness error by ensuring that the inversion parameters used in this work were consistent. Unusual ground conditions completely avoided due to the choice of the survey period made. Immediate 3D geology for profiles laid across the strike of lengthy geological structures which could have a basic limitation of delineating such structures. Res2DInv program might have an assumption of a 2D subsurface model which may not be completely true.

Interpretation and Discussion

Expertise in the interpretation of geophysical data is a cardinal factor which is usually developed with time (Dobrin, 1978). Also, the essentials for correct interpretation must basically include adequate knowledge of the nature of data collected and processed (Koch, 2004).Hence, it was ensured that the interpretation of the 2D electrical imaging pseudosections from this work was based on the knowledge of the geology of the study area, previous work done around the study area and some published standard resistivity values. These would lend logical support to all interpretations hence aid concise discussion and conclusions on the processed data from this study.

Interpretation in this survey's data is derived from the resistivity values obtained from previous works at different areas of Nnewi–Oba (Obiabunmo*et. al.* 2014), its environs (Fatoba*et al*, 2013, Ramel*iet al.*, 2016, Bayowa, 2015, Agbo, 2008.) and some standard resisivities from Telford *et al.*,(1990) and IEEE (2011). The summary of the published resistivity values and interpretations by these authors which are also adopted for interpretation in this study are given in Table 3.

Table 3: Resistivity values adopted for data interpretation of delineated 2D model sections

Soil and Rock Type	Range of Published Resistivity Range (Ωm)	Contributing Authors and year of Publication
Topsoil: Lateritic	32 - 1961	Fatoba, *et. al.,* (2013), Obiabunmo, *et. al.,* (2014), IEEE (2011)
Saturated soil	4 – 98	Obiabunmo, *et. al.,* (2014),
Clay	1 – 100	Fatoba, *et. al.,* (2013), Obiabunmo, *et. al.,* (2014), IEEE (2011), Rameli*et. al.,* (2016), Telford *et al.,* (1990), Agbo (2008)
Sandy clay	40 - 300	IEEE (2011), Rameli*et. al.,* (2016)
Clayey sand	50 - 1500	Obiabunmo, *et. al.,* (2014), IEEE (2011),
Sandstone	1 - 5000	Obiabunmo, *et. al.,* (2014), IEEE (2011), Rameli*et. al.,* (2016), Telford *et al.,* (1990),
Dry sandstone	4256 - 29916	Obiabunmo, *et. al.,* (2014), Agbo (2008)
Weathered basement	50 – 500	Agbo (2008)

The 2D resistivity models obtained from the data processing shows that the shallow-surface lithology at the vicinity of the gully has resistivity in a wide range of about $1\ \Omega m - 53{,}500\ \Omega m$ (Figures 9-15). Interpretation in this study is based on the publications of Fatoba, *et. al.*(2013), Obiabunmo, *et. al.* (2014), IEEE (2011), Rameli*et. al.*(2016), Telford*et al.*(1990) and Agbo (2008). However ambiguity in interpretation is inevitable due to overlapping of resistivity values. The resistivity range $1\ \Omega m - 53{,}500\ \Omega m$ modelled for subsurface materials encompasses those of clay 1-100 Ωm, 40Ωm – 300 Ωm,saturated soil 4Ωm – 98 Ωm, sandstone 1Ωm – 5000Ωm and weathered basement (50-500 Ωm). Table 4 shows the summary of the predominance for the delineated and interpreted subsurface materials at the study site. It can be observed very obviously from the table that the predominant near-surface soils at the site include; clay and sandy clay of various grades. That is, at higher consolidation, these could be inferred to be conglomerate or to be shaley. Also predominant at the vicinity are soil and sandstones of various grades of saturation. While the saturation of the predominant soils and rocks is relatively higher at profiles P1, P3, P4 and P7 (figures 9, 11, 12 and 15), very high dry soils marked by high margin of resistivity hence suspected to be predominantly very dry highly consolidated soils and rocks. Nevertheless, guided by the knowledge of the geology of the area, the very high resistivity range mapped in this study is invariably far from being occurrence of fracture or weathered basement let alone the basement itself.

Structurally, the shallow-surface contour colorations are predominantly heterogeneous, showing high variability at low contour intervals. Uniformity in the formation of layered subsurface of the soil is not observed common among the delineated profiles (especially at P1, P5 and P7) (figures 9, 13 and 15). However, relative uniform layers could be observed at some of them (P2, P3, P4 and P8) (figures 10, 11, 12 and 16) also, none of these is noticeably a dipping layer. Remarkably but in minority, structural features suspected to be fractured zone and anticline could be observed at the base of profiles P4 and P8 (figures 11 and 16) respectively).

Table 4: Summary of predominance levels for the delineated and interpreted subsurface materials at the study site

Profile Identity and Average Resistivity Range(Ωm)	Predominant Lithological Interpretation (most Probable)							Structural features
	Clay	**Sandy Clay**	**Clayey Sand**	**Saturated Soil**	**Sandstone (dry)**	**Saturated Sandstone**	**Lateritic soil (weathered)**	
P1 (50-8,000)	√√	√	√√√	√√	×	××	√	×××
P2 (40-22,000)	√√√ (saturated intercalates)	√	√√√	√√√	×××	××	√√	×××
P3 (200-6,300)	√ (minor parches at topsoil)	×	√√	×	×	√ (minor at depths)	√√√	×××
P4 (10-7,000)	√√	√√	√√√	√√	××	√√ (minor at base)	√√ (minor at base)	Suspected shallow fracture at base of 2D model
P5 (1-6,500)	√ (saturated intercalate)	√√√	√√	√√	×××	××	×××	Suspected concrete, high resistive shallow rooted boulder
P6 (1-53,5000)	√√√	√√√	√√	√	×××	√√ (suspected minor occurrence)	√√	Double intrusion of clayey sand
P7 (150-5,000)	××	√	√√√(appear intrusive)	×	××	√√ (suspected occurrence at topsoil)	√√ (suspected occurrence at topsoil)	×××
P8 (10-30,000)	√√ (fairly at topsoil)	√√	√√√	√√ (fairly at topsoil)	√√√ (flanked by clayey sand)	√ (fairly at topsoil)	√√ (flanked by clayey sand)	anticline (suspected to be dry sandstone)

(Legend: √√√:- predominant, √√:- fairly predominant, √:- insignificantly present; ×××:- significantly absent, ××:- partially absent and ×:- totally absent)

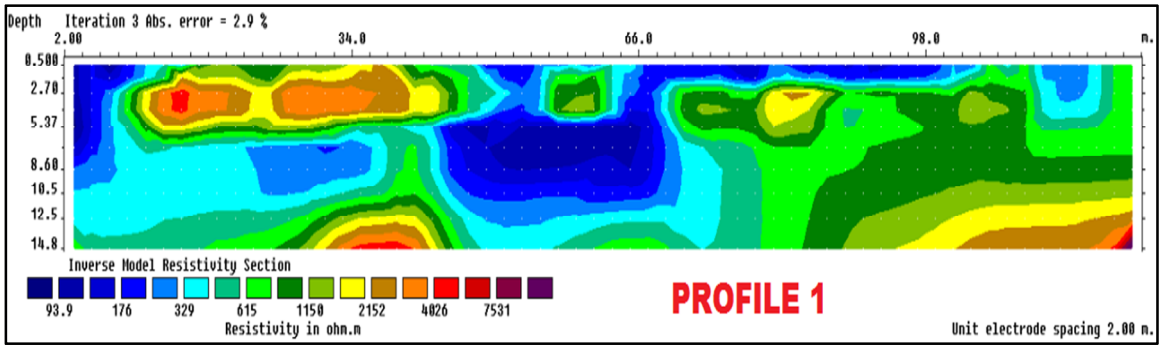

Fig.9: Results of 2D Inversion of the Wenner Array data along Profile 1

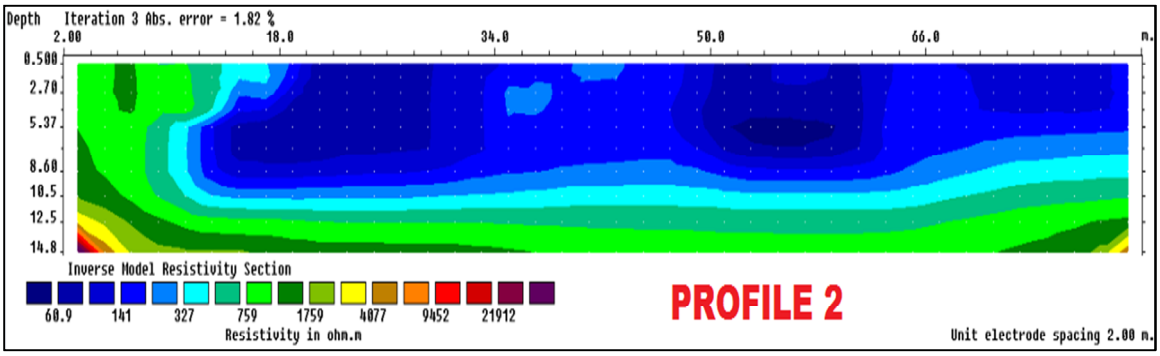

Fig.10: Results of 2D Inversion of the Wenner Array data along Profile 2

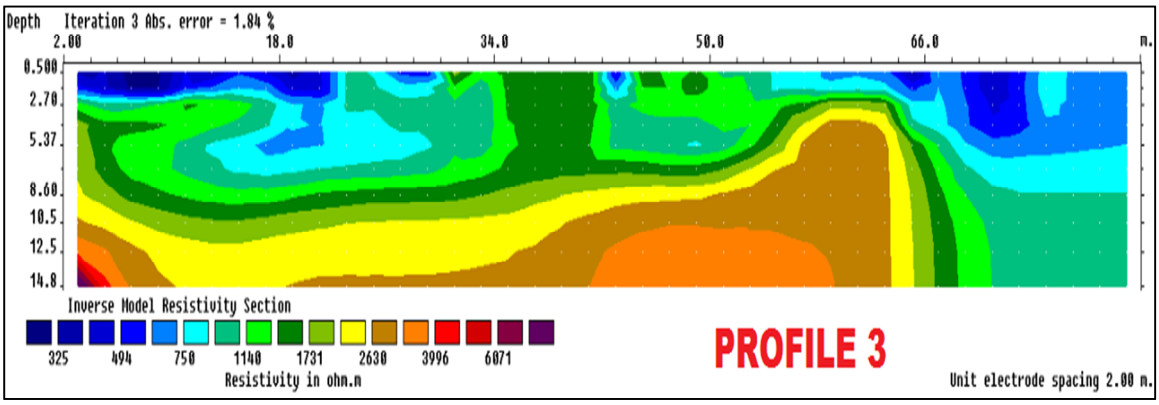

Fig.11: Results of 2D Inversion of the Wenner Array data along Profile 3

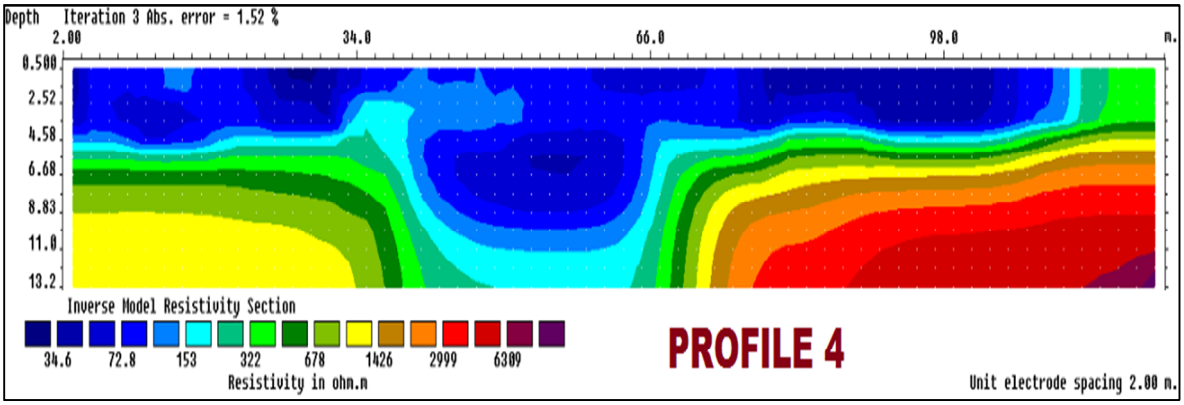

Fig.12: Results of 2D Inversion of the Wenner Array data along Profile 4

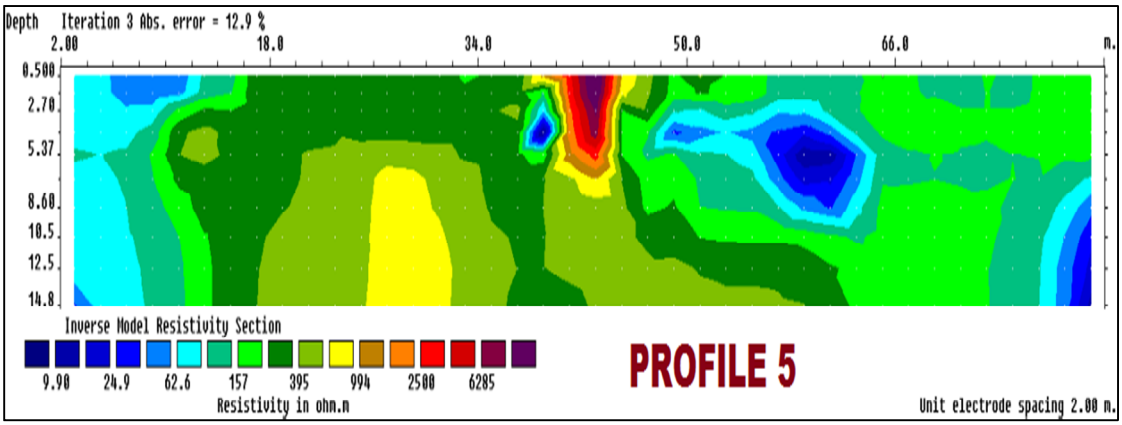

Fig.13 :Results of 2D Inversion of the Wenner Array data along Profile 5

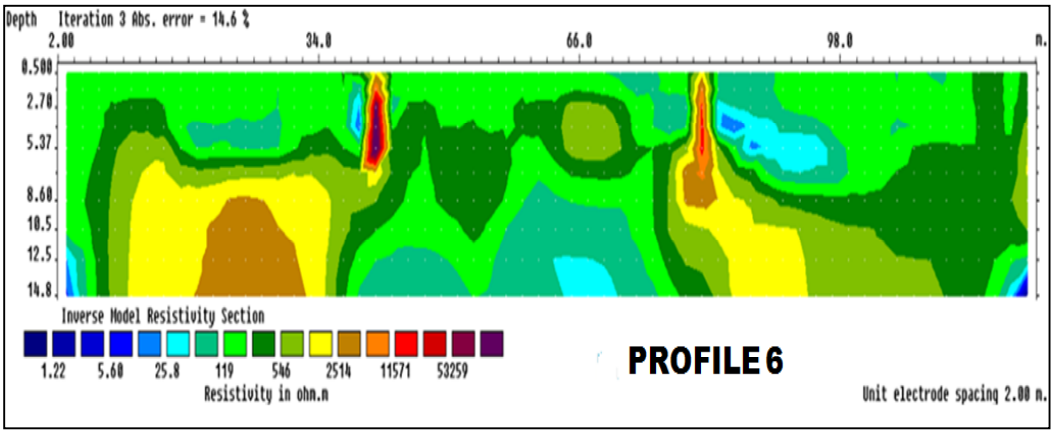

Fig.14: Results of 2D Inversion of the Wenner Array data along Profile 6

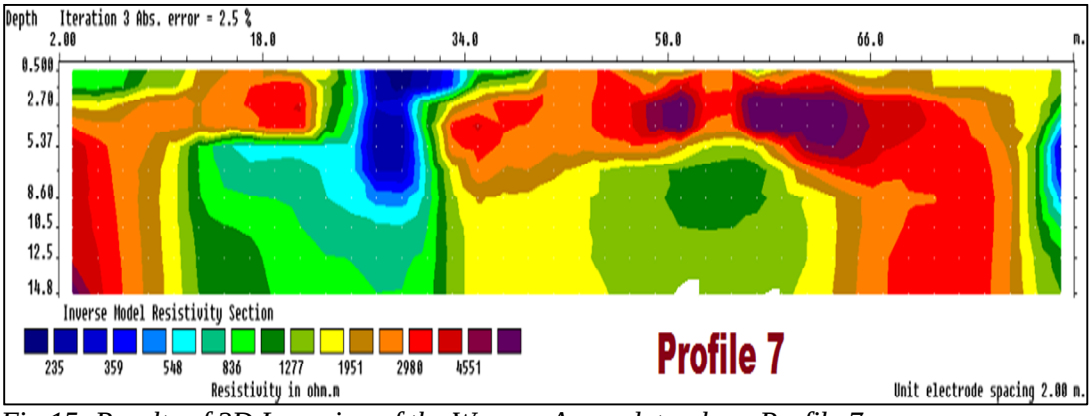

Fig.15: Results of 2D Inversion of the Wenner Array data along Profile 7

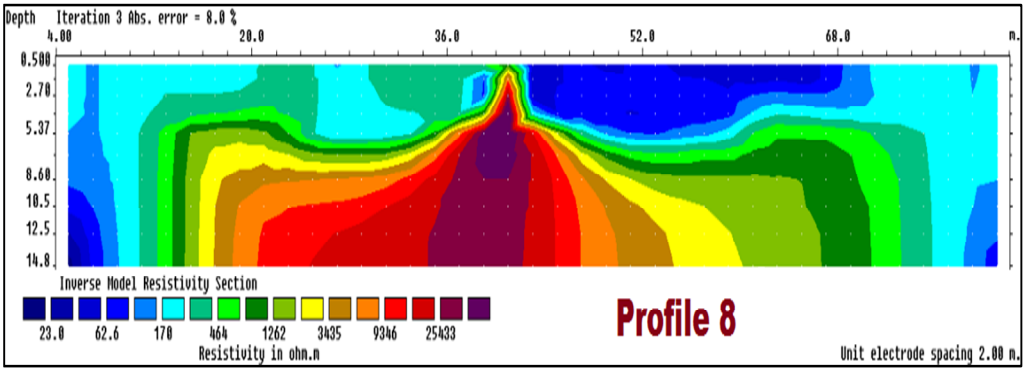

Fig.16: Results of 2D Inversion of the Wenner Array data along Profile 3

Implications and dangers of clayey soil at shallow and foundation depths of buildings includes seasonal swell and shrinkages leading to fracturing of groundsurface and deepening fractal cracks, fracturing of superstructures' foundation, increment of weak zones at shallow subsurfaces and creepy movements due to seasonal volume changes of the clayey soils (Egwuonwu *et al.*, 2011). Moreover, delineating a high level of saturation retention in soils at near-surface even at the peak of dry season when the survey was carried would mostly likely trigger both sub-structural and superstructures' failure thereat. Doubtlessly, the weakness and resultant failure of the subsurface and superstructures at the vicinity would be exacerbated more grossly when rainy season fully comes. This is the crux of the danger of the active sub-structure' leading to superstructures' failures at Uruagu-Nnewi gully site (Figures 3 and 4). Fractured subsurface marked with relatively low resistivity and unconsolidated zones flanked by relatively high resistivity and consolidated zones places superstructures in danger of foundation based cracks and failure. Also, the occurrence of syncline or anticline structures at shallow depths would place

high rise superstructures in danger of leaning and failure (Egwuonwu *et al.,* 2011). Meanwhile, for the fact that these features of clay enrichment, weak zone, saturation retention, occurrence of fracture and anticline occur at gully walls and the immediate surroundings of the Uruage-Nnewi active gully site, calls for eminent attention. Hence, its urgency is a matter of great conscientious concern to geoscientists and environmental civil engineers for propounding proactive remedy for the menace.

Conclusions and Recommendations

Based on the interpretation given in the foregoing, it is conceivable to make conclusions and inferences based on the study in the foregoing. Having delineated from processed and modeled data, the range of resistivity 1 Ωm to about 25,500Ωm is been based upon for meaningful interpretations. Of this wide range, clayey sand$(50-1{,}500\ \Omega m)$, sandy clay$(40-300\ \Omega m)$,and saturated soils of various grades$(4-98\ \Omega m)$were observed to be most prominent at the gully's vicinity. The shallow surface resistivity distribution is heterogeneous hence, layering at the shallow depths is very minor. Due to the occurrences of intercalates, suspected fractures, the subsurface could be considered to be characterized by undulations which enhances saturation in rainy seasons, hence weakens the shallow surface columns. Both transverse and longitudinal profiles to the strike of the gully were predominantly characterized by very low resistivity values interpreted to be clayey heterogenous permeable and expansive soils hence making the vicinity to be prone to the failure of both subsurface structures and superstructures in the area. The interpreted ERT tomograms obtained suggest that the active landslides at the gully's vicinity are most probably aggravated to differential saturation of the gully's vicinity hence, leading intermittent abrupt landslide and failures.

The findings of this study would reveal how eminent the management of Uruagu, Nnewi active gully/landslide site is. It is suspected that previous water courses over the decades have most probably deformed the general topography of the site and its environs hence resulted to the notable deep gully. Previous use of the site and lack of proper and adequate checks of erosion paths weren't recorded for proper inference. Dumping of refuse into the gully noticed in recent time would rather prolong retention of water on the delineated weak subsurface at the vicinity of the gully. Therefore, while 3D geophysical imaging is recommended for further study of the near-surface, boreholes logs and test pits would properly fit in as complementary works upon this. Environmentalists in geography, geology and civil engineering professions should be encouraged to seek proactive solutions to the menace. Meanwhile, Nigeria government should, as a matter of national priority and urgency, enforce prohibition of further erection of superstructures across, along and upon the immediate vicinity of such active gullies sites.

Acknowledgement

The authors are immensely grateful to the Centre for Geodesy and Geodynamics, Toro, Bauchi State for providing the field equipment used for the study.

References

Abdulfatai,I. A., Okunlola, I. A., Akande, W. G., Momoh,L. O., & Ibrahim, K. O. (2014). Review of Gully Erosion in Nigeria: Causes, Impacts and Possible Solutions. *Journal of Geosciences and Geomatics, Science and Education Publishi, 2(3) 125-129. DOI:10.1 2691/jgg-2-3-8*

ABEM Instrument AB, (2010): TerrameterSAS1000/4000 LUND Imaging System Introduction Manual.

Agbo, C. (2014). 2-D Electrical Resistivity Imaging around the collapsed buildings of the housing estate at Barnawa-Narayi junction, Kaduna, Kaduna state.Geophysics Department of Physics Faculty of Science, Ahmadu Bello University, Zaria.

Bayowa, G.O., Falebita, D.E. and Adegboyega R. O. (2015). "Surface DC resistivity survey of contamination Beneath Ido-Osun dumpsite, southwestern Nigeria" *Geophysical International Vol.* 54-4: 343-352

Claerbout, J. andMuir, F. (1973) "Robust Modeling with Erratic Data," *Geophysics*, Vol. 38, (5), pp. 826-844

Dobrin, M. B. (1978). Introduction to Geophysical Prospecting (*3rd Edition*), McGraw-Hill, New York. p.630

Egboka B. C. and Okoyeh E. I., (2016).The Impacts and Implications of Anthropogenic Forces on the Unstable Geologic Platform in Parts of Anambra and Imo States Southeastern, Nigeria, *International Journal of Environmental Protection and Policy*. 4(4),104-110. doi: 10.11648/j.ijepp.20160404.1.

Egboka, B.C.E and Nwankwo, G.I. (1982). The Agulu-Nanka gully: An explanation for its origin. Quarterly*Journal for Engineers and Geologist,* (8): 54-61

Egwuonwu, G.N. (2012). "Application of Geophysical Imaging in Investigation of Structural Failure of Buildings: Case Study of Three Building Sites in Zaria Area, Northwestern Nigeria". *Pacific Journal of Science and Technology*. 13(1):580-589.

Egwuonwu, G.N., Ibes.o. andOsazuwaI.B.(2011). "Geophysical assessment of Foundation depths around a leaning Superstructure in Zaria Area, Nigeria using electrical resistivity tomography".*Pacific Journal of Science and Technology.* 12(2):472-480.

Ezechi, J.I and C.O. Okagbue (1989), a genetic classification of gullies in easternNigeria and its implications on control measures. Journal of African EarthSciences, 9, pp 711-718.

Ezeigwe, P. C. (2015). Evaluation of the Socio-Economic Impacts of Gully Erosion in Nkpor and Obosi.*Civil and Environmental Research, 7*(7), 2225-0514.Retrieved June 5, 2017.

FatobaJ.O., Salami B.M.andAdesida A. (2013). "Structural failure investigation using electrical resistivity method: A case study of AmaforIhuokpala,Enugu, Southeastern Nigeria" Journal of Geology and Mining Research Vol.5(8),p.208-215ISSN2006–9766 http://www.academicjournals.org/JGMR.

Frankl, A., Deckers, J., Moulaert, L., Van Damme, A., Haile, M., Poesen, J., Nyssen, J. (2013). Integrated solutions for combating gully erosion in areas prone to soil piping: Innovations from the drylands of northern Ethiopia. *Land Degradation and Development*: 2014. DOI: 10.1002/ldr.2301

Google Maps, (2018).*Map of Nnewi, Anambra*, 1:1.500. Google Maps (online) Available through: Anglia Ruskin University Library <http://libweb.anglia.ac.uk> (Accessed 31 August 2018.

IEEE 142, (2007).Earth Rod Electrode Resistance. IEEE Recommended Practice for Grounding of Industrial and Commercial Power Systems (Green Book).*Institute of Electrical and Electronics Engineers, Inc.* IEEE Std 142™-2007

IEEE 142, (2011) Earth Rod Electrode Resistance of Industrial and Commercial Power System (Green Book)

Igbokwe, J. I., Akinyede, J. O. Dang, B.T. Alaga, T. M. N. Ono, M. N. and .Nnodu, V. C.(2008). Mapping and Monitoring of the impact of gully erosion in southeastern Nigeria with satellite remote sensing and geographic information system: The International Archives of the Photogrammetry. *International Journal of Environmental Sciences* Vol. 2(2) 8pp.

Jadwiga A. Jarzyna, Jerzy Dec, Karczewski J, Porzucek S, Sylwia T, Wojas A and Ziętek J (2012). Geophysics in Near-Surface Investigations, New Achievements in Geoscience, Dr. Hwee-San Lim (Ed.), ISBN: 978-953-51-0263-2, InTech, Available *from: http://www.intechopen.com/books/new-achievements-in-geoscience/geophysics-in-near-surface-investigations*

Koch, K. M. (2004). Application of electrical resistivity tomography (ERT) together with tracer data to identify hydrological process areas at a surface water / groundwater test site. *Institutfür Hydrologie, Albert-Ludwigs Universität Freiburg i. Br*. St. Wilhelm, Black Forest Mountains, Germany

Loke, M.H. (2004), "Tutorial: 2D and 3D electrical Imaging Surveys" Copyright 1996-2004 136p

Nelson, S. A., (2015). Mass Movements- Physical Geology. Tulane University. *Retrieved from: https://www.tulane.edu/~sanelson/eens1110/massmovements.htm*

Obiabunmo, O. C., Umego, M. N., Obiekezie, T. N., and Chinwuko, A. I. (2014). "Application of electrical resistivity method for groundwater exploration in Obaand environs, Anambra state, Nigeria.Adv. Phys. Theor. Appl.37, 19–29

Obiadi, I.I., Nwosu, C.M.,Ajaegwu, N.E.Anakwuba.E.K, Onuigbo.N.E, Akpunonu.E.O, and Ezim, O.E. (2011). Gully Erosion in Anambra State, South East Nigeria: Issues and Solution. *International Journal of Environmental Sciences, 2(2)0976 – 4402*

Onochi N. E. and Ibearugblem O. H. (2012).Geophysical and Hydrogeological Investigation for Groundwater at UmumejiakuUruagu Nnewi, Nnewi-North Local Government of Anambra State.*Bookman International Journal of Mechanical and Civil Engineering,* 1(2)41-43,ISSN No. 2319-4286.

Riyadh, R. Y., Ros F. M., Samsudin H. T., (2014). Geohazard Assessment of Carbonate Karst Features in Construction Sites by Application of Combined techniques in (Kinta Valley) Perak, Peninsular Malaysia. *International Journal of Advanced Scientific and Technical Research*, 6(4)366-406, ISSN 2249-9954. Available online on http://www.rspublication.com/ijst/index.html

Robert, L. S. and Lynn, M. H., (2001).Socioeconomic and Environmental Impacts of Landslides in the Western Hemisphere.*U.S.Geological Survey, Denver, Colorado 80225. Open-File Report 01-276.*

Runqiu, H., and Weile, L., (2011). Formation, distribution and risk control of landslides in China. *Journal of Rock Mechanics and Geotechnical Engineering*, 3 (2): 97–116

Telford, W. M. Geldart, L. P. Sherif, R. E. and Keys, D. A., (1990).Applied Geophysics. 2nd Edition, Cambridge University Press. New York.

Uzoije, A. P., Uzoigwe L., Otuonye E., Kamalu C. O. and Onunkwo-Akunne, A. (2013). Modeling Lateral Distribution of Heavy Metal and Bio-accumulation in Earthworm in the Varying Acidic Surface Horizon of Waste- Polluted Soil, *International Journal of Energy Engineering*, 3(2)45-54.doi: 10.5923/j.ijee.20130302.02.

Watkins, A. and Hughes, S**., (**2000). Landslides, Slope Failure, and Other Mass Wasting Processes. Environmental Geology: Chapters 6, p. 131-160 in textbook, Keller, 2000. Retrieved on the 14th of Aug. 2017 from http://geology.isu.edu/wapi/EnvGeo/EG4_mass_wasting/EG_module_4.htm

Wolke, R. and Schwetlick, H. (1988) "Iteratively Reweighted Least Squares: Algorithms, Convergence Analysis, and Numerical Comparisons" *SIAM Journal on Scientific and Statistical Computing* 9(5).